CHEMISTRY
AN ASIAN JOURNAL

DOI: 10.1002/asia.200600358

Shape- and Functionality-Controlled Organization of TiO_2–Porphyrin–C_{60} Assemblies for Improved Performance of Photochemical Solar Cells

Taku Hasobe,[a, b] Shunichi Fukuzumi,*[a] Shigeki Hattori,[a] and Prashant V. Kamat*[b]

Abstract: Shape- and functionality-controlled organization of porphyrin derivatives–C_{60} supramolecular assemblies using TiO_2 nanotubes and nanoparticles has been achieved for the development of photochemical solar cells. The differences in the efficiency of light-energy conversion of these solar cells are explained on the basis of the geometrical orientation of the porphyrins with respect to the TiO_2 surface and the supramolecular complex formed with C_{60}. The maximum photon-conversion efficiency (IPCE) of 60% obtained with TiO_2 nanotube architecture is higher than the value obtained with nanoparticle architecture. The results presented in this study show the importance of substrate morphology in promoting electron transport within the mesoscopic semiconductor film.

Keywords: electrophoresis · fullerenes · nanotubes · organic solar cells · photoelectrochemistry · porphyrin

Introduction

Dye-sensitized photoelectrochemical cells have emerged as a promising alternative for the development of next-generation solar cells.[1–5] These cells have been shown to deliver power with efficiencies greater than 11%. The low cost and ease of manufacturing of these cells has led to much new effort to improve their performance. The dye-sensitized solar cells investigated so far involve high-surface-area mesoscopic TiO_2 films modified with light-absorbing dye molecules. Despite their random geometry and orientation, these dye-modified TiO_2 films provide the basis for achieving light-induced charge separation and transport of charge carriers to generate the photocurrent. An important class of organic dyes that has shown promise for the sensitization of TiO_2 is porphyrin and its derivatives.[6–12] The energy-conversion efficiency of solar cells that employ porphyrin as the sensitizer was recently increased up to more than 5%.[11] However, problems remain for the further improvement of this property.

Anchoring sensitizer molecules to nanostructured semiconductor film is a crucial step in maximizing the energy-conversion efficiency of dye-sensitized solar cells. The choice of linker molecules paves the way for achieving higher surface coverage, increased stability, minimal desorption, and even distribution of the sensitizer molecules with minimal aggregation. Anchoring groups such as phosphonates or carboxylic acid derivatives form strong covalent bonds or facilitate charge-transfer (CT) interaction with the metal oxide surface and provide the necessary electronic coupling to maximize the charge-injection efficiency. Multiple linker groups attached to a single chromophore can mean the introduction of additional organizational features. For example, Galoppini and co-workers[1,13,14] have developed rigid tripodal linkers that anchor to semiconductor nanoparticles. Tripodal linkers with three points of attachment and a fourth rigid arm to carry the chromophore provided large targets for attaching the sensitizer.

Supramolecular assemblies of porphyrin and C_{60} have been characterized to explore CT interactions and photoinduced electron-transfer processes.[15–17] The hierarchical organization of these assemblies is an important aspect for

[a] Dr. T. Hasobe,[+] Prof. S. Fukuzumi, S. Hattori
Department of Material and Life Science
Graduate School of Engineering, Osaka University
Suita, SORST, Japan Science and Technology Agency
Osaka 565-0871 (Japan)
Fax: (+81) 6-6879-7370
E-mail: fukuzumi@ap.chem.eng.osaka-u.ac.jp

[b] Dr. T. Hasobe,[+] Prof. P. V. Kamat
Radiation Laboratory, Departments of Chemistry & Biochemistry and Chemical & Biomolecular Engineering
University of Notre Dame
Notre Dame, Indiana 46556 (USA)
Fax: (+1) 574-631-8068
E-mail: pkamat@nd.edu

[+] Current address: School of Materials Science
Japan Advanced Institute of Science and Technology (JAIST)
Nomi, Ishikawa, 923-1292 (Japan)

Supporting information for this article is available on the WWW under http://www.chemasianj.org or from the author.

maximizing the efficiency of light-energy conversion in photoelectrochemical cells. A quaternary-organization approach is effective for assembling gold nanoparticle–porphyrin–C_{60} hybrid systems on electrode surfaces and maximizing the efficiency of light-energy conversion.[18–21] A photoinduced electron transfer between the excited state of porphyrin and C_{60} results in the formation of $C_{60}^{\bullet-}$, which in turn transfers electrons to the collecting surface of the electrode to generate the photocurrent. The architecture of the ordered assemblies facilitates the stabilization of electron-transfer products and thus enables maximum efficiency of light-energy conversion. Such an organizational approach has yet to be explored fully in dye-sensitized solar cells.

Herein, we chose the monocarboxy- and tetracarboxy-substituted porphyrins 5-[4-benzoic acid]-10,15,20-tris[3,5-di-*tert*-butylphenyl]-21*H*,23*H*-porphyrin (Ar-H_2P-COOH), 5-[4-benzoic acid]-10,20-di[3,5-di-*tert*-butylphenyl]-21*H*,23*H*-porphyrin (H-H_2P-COOH), and 5,10,15,20-tetra[4-benzoic acid]-21*H*,23*H*-porphyrin (H_2P-4COOH) to bind to the TiO_2 surface and to orientate the sensitizer molecules in a perpendicular and planar geometry (Figure 1). We selected spherical nanoparticles as well as nanotubes of TiO_2 to compare the geometric effect of oxide support for attaining different hierarchical configurations of light-harvesting assemblies. The porphyrins anchored to the TiO_2 nanoparticles and nanotubes, when in contact with C_{60}, underwent CT interactions and provided a secondary organization of these assemblies. Because of the nature of the geometrical orientation of the porphyrins with respect to the TiO_2 surface, we obtained two different secondary organization structures. A tertiary organization of the TiO_2–porphyrin–C_{60} assemblies on the electrode surface could further assist in the elucidation of the effect of orientation on photoconversion efficiency. The structural differences, such as between nanoparticles and nanotubes, and the substituent effects of the porphyrins for the organization of donor and acceptor moieties have a great effect on the photoelectrochemical properties. Ways to improve the photoelectrochemical behavior of the composite films of porphyrin–fullerene clusters organized by TiO_2 semiconductor materials are discussed herein.

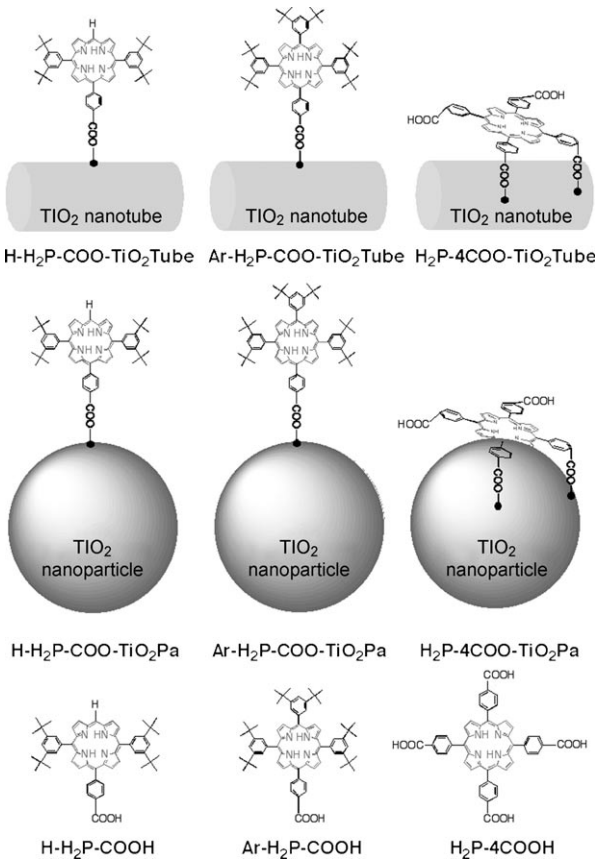

Figure 1. TiO_2 nanotubes and nanoparticles modified with porphyrin dyes and the reference compounds employed in this study.

Results and Discussion

Preparation and Morphology of TiO_2–Porphyrin–Fullerene Assemblies

Porphyrins and C_{60} are soluble in nonpolar solvents such as toluene, but much less soluble in polar solvents such as acetonitrile.[22,23] By proper choice of polar to nonpolar solvent, we achieved controlled aggregation in the form of composite nanoclusters. Detailed information on composite nanoclusters of porphyrins and C_{60} has been described elsewhere.[22] TiO_2 nanoparticles were electrophoretically deposited onto the electrode in suspended solution.[24–26] Upon subjecting the resulting cluster suspension to a high electric direct current (dc) field (500 $V\,cm^{-1}$), mixed porphyrin-modified TiO_2 nanotubes or nanoparticles and fullerene clusters (denoted $(H_2P\text{-}COO\text{-}TiO_2Tube + C_{60})_n$ and $(H_2P\text{-}COO\text{-}TiO_2Pa + C_{60})_n$, respectively) were deposited onto an optically transparent electrode (OTE) of a nanostructured SnO_2 electrode (OTE/SnO_2) to afford the modified electrode (denoted OTE/SnO_2/$(H_2P\text{-}COO\text{-}TiO_2Tube + C_{60})_n$ and OTE/SnO_2/$(H_2P\text{-}COO\text{-}TiO_2Pa + C_{60})_n$, respectively). As the deposition continued, we observed decoloration of the solution accompanied by coloration of the electrode connected to the positive terminal of the dc power supply. A mixed cluster suspension of porphyrin-modified TiO_2 nanotubes (Ar-H_2P-COO-TiO_2Tube, H-H_2P-COO-TiO_2Tube, H_2P-4COO-TiO_2Tube) and nanoparticles (Ar-H_2P-COO-TiO_2Pa, H-H_2P-COO-TiO_2Pa, H_2P-4COO-TiO_2Pa) and C_{60} were prepared in the total concentration range of 0.025–0.13 $mmol\,dm^{-3}$ (molecular ratio of $H_2P/C_{60} = 1{:}5$) in acetonitrile/toluene (3:1 *v*/*v*). In this case, the mixed clusters were first prepared by using different amounts of H_2P on the TiO_2 nanotubes or nanoparticles and C_{60} to maintain their molar ratio as 1:5. Figure 2A and B show the transmission electron microscopy (TEM) images of H-H_2P-modified TiO_2 nanotubes and nanoparticles (H-H_2P-COO-TiO_2Tube and H-H_2P-COO-TiO_2Pa), respectively. These two images show the distinguishable structural features, that is, the tubular and particle structures of the H_2P-modified TiO_2 precursors employed prior to complexation with C_{60}. Any aggregation

CHEMISTRY
AN ASIAN JOURNAL

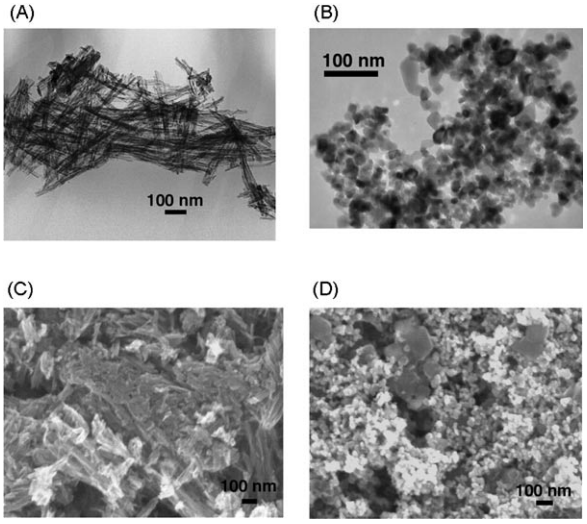

Figure 2. (A) TEM image of H-H_2P-COO-TiO_2Tube, (B) TEM image of H-H_2P-COO-TiO_2Pa, (C) SEM image of OTE/SnO_2/(H-H_2P-COO-TiO_2Tube + C_{60})$_n$ ([H_2P] = 0.025 mM, [C_{60}] = 0.13 mM), (D) SEM image of OTE/SnO_2/(H-H_2P-COO-TiO_2Pa + C_{60})$_n$ ([H_2P] = 0.025 mM, [C_{60}] = 0.13 mM).

of H-H_2P-COO-TiO_2Pa and H-H_2P-COO-TiO_2Tube seen on the TEM grid is likely to arise from close-packing of the molecules. Figure 2C and D show the scanning electron microscopy (SEM) images of OTE/SnO_2/(H-H_2P-COO-TiO_2Tube + C_{60})$_n$ and OTE/SnO_2/(H-H_2P-COO-TiO_2Pa + C_{60})$_n$, respectively. The TiO_2 nanotubes and nanoparticles assembled on the electrode surface as packed nanostructures. Comparison of the SEM images with the TEM images demonstrate that composite molecular clusters with TiO_2 nanotubes or nanoparticles as deposited onto OTE/SnO_2 electrodes retain their morphology without exhibiting significant bundling effects or particle growth.

Absorption Properties of TiO_2–Porphyrin–Fullerene Assemblies on OTE/SnO_2 Films

The absorption spectra of a few representative electrodes are shown in Figure 3 (spectra a, b, and c). The reference spectra of pristine C_{60} and H-H_2P-COOH in toluene are also shown (spectra d and e). Compared to the reference spectra, the spectra of the supramolecular assemblies on the OTE/SnO_2 electrodes show broad absorption. In particular, the spectrum of OTE/SnO_2/(H-H_2P-COO-TiO_2Pa + C_{60})$_n$ (spectrum b) becomes much broader than that of OTE/SnO_2/(H-H_2P-COO-TiO_2Pa)$_n$ (spectrum a). Along with scattering effects, the CT complexation between porphyrin and fullerene[20] is expected to dominate the absorption in the red region.

Figure 4 shows the absorption spectra of the porphyrin, C_{60}, and their mixture, for the examination of the CT absorption between porphyrin and C_{60}. The CT absorption is obtained by subtracting the spectra of both H-H_2P-COOMe (5-[4-methoxyphenyl]-10,20-di[3,5-di-*tert*-butylphenyl]-21*H*,23*H*-porphyrin) (spectrum b) and C_{60} (spectrum c) from that

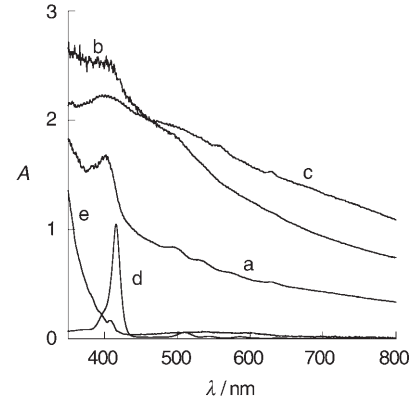

Figure 3. Absorption spectra of a) OTE/SnO_2/(H-H_2P-COO-TiO_2Pa)$_n$ ([H_2P] = 0.025 mM), b) OTE/SnO_2/(H-H_2P-COO-TiO_2Pa + C_{60})$_n$ ([H_2P] = 0.025 mM, [C_{60}] = 0.13 mM), c) OTE/SnO_2/(H-H_2P-COO-TiO_2Tube + C_{60})$_n$ ([H_2P] = 0.025 mM, [C_{60}] = 0.13 mM), d) H-H_2P-COOH in toluene (5 μM), and e) C_{60} in toluene (15 μM).

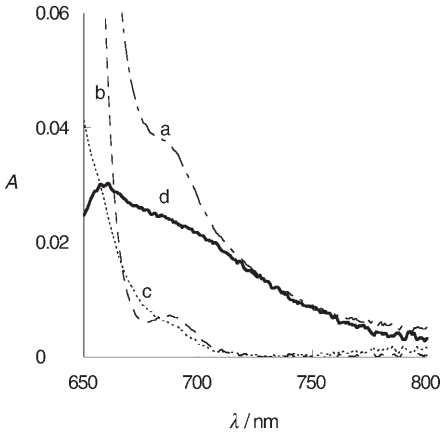

Figure 4. Absorption spectra of a) mixed 1.0 mM H-H_2P-COOMe (5-[4-methoxyphenyl]-10,20-di[3,5-di-*tert*-butylphenyl]-21*H*,23*H*-porphyrin) and 5.0 mM C_{60}, b) 1.0 mM H-H_2P-COOMe, and c) 5.0 mM C_{60} in *o*-dichlorobenzene. d) CT absorption of 1.0 mM H-H_2P-COOMe and 5.0 mM C_{60}, obtained by subtracting the absorption of b) and c) from a).

of H-H_2P-COOMe and C_{60} (spectrum a). The broad absorption in the visible and near-IR regions is characteristic of the π complex formed between porphyrins and fullerenes.[20,27,28] CT-type interactions in the π complex between porphyrin and fullerene molecules may be responsible for the long-wavelength absorption of the composite clusters in Figure 3, in which the spectra of the TiO_2–porphyrin–fullerene composites (Figure 3, spectra b and c) are much broader than those of TiO_2–porphyrin alone (Figure 3, spectrum a). Similar CT interactions leading to such an extended absorption have been observed for porphyrin–C_{60} dyads linked at close proximity.[29] Thus, we can control the three-dimensional array of porphyrins and C_{60} molecules by TiO_2 semiconductor nanomaterials, and the absorption arising from the CT interaction extends the light-harvesting capability in the entire visible and near-IR region.

Taking into consideration the above results, we suggest that supramolecular assemblies between porphyrins and fullerenes using TiO_2 nanotubes and nanoparticles are formed as shown in Figure 5. The question now is what effect the porphyrin–fullerene assemblies using TiO_2 nanotubes or nanoparticles have on the photoelectrochemical properties.

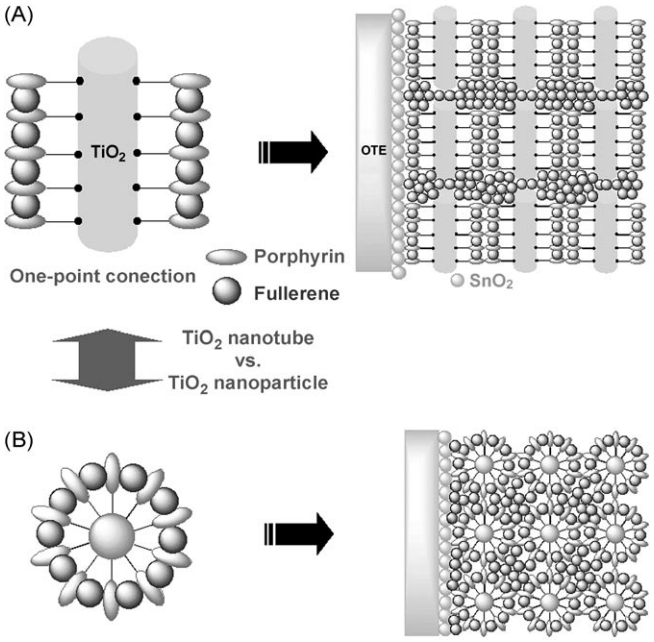

Figure 5. Diagrammatic summary of the organization between porphyrin and fullerene moieties using TiO_2 nanotubes (A) and nanoparticles (B).

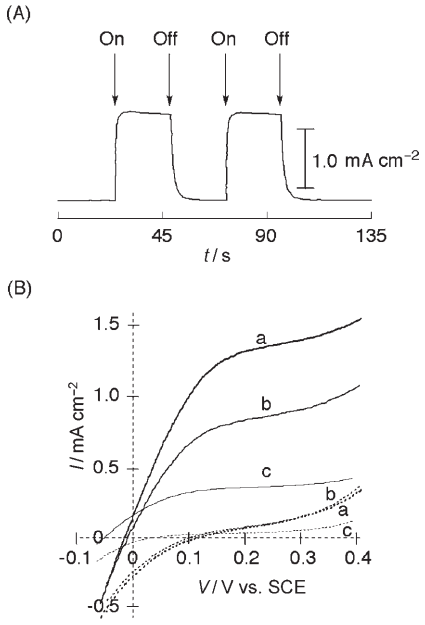

Figure 6. (A) Short-circuit photocurrent response of OTE/SnO_2/(H-H_2P-COO-TiO_2Tube+C_{60})$_n$ at an applied bias potential of 0.2 V vs. SCE; input power: 27.8 mW cm^{-2} under white-light illumination ($\lambda > 400$ nm). (B) Current–voltage (I–V) characteristics (with SCE reference electrode) of a) OTE/SnO_2/(H-H_2P-COO-TiO_2Tube +C_{60})$_n$, b) OTE/SnO_2/(H-H_2P-COO-TiO_2Pa+C_{60})$_n$, and c) OTE/SnO_2/(H-H_2P-COO-TiO_2Pa)$_n$ under illumination of white light ($\lambda > 400$ nm). The solid and dotted lines correspond to the photocurrent and dark current, respectively. [H_2P]= 0.025 mM, [C_{60}]=0.13 mM; electrolyte: 0.5 M NaI and 0.01 M I_2 in acetonitrile; input power: 27.8 mW cm^{-2}.

Photoelectrochemical Properties of OTE/SnO_2 Films with TiO_2–Porphyrin–Fullerene Assemblies

The monocarboxylic acid substituted porphyrins were attached to the TiO_2 surface by a single carboxylic acid linker (Figure 1), thus stretching out the porphyrin moiety perpendicular to the TiO_2 surface. The complexation of C_{60} molecules between the two porphyrin moieties provides additional organization on the particle surface (Figure 5). Higher-level hierarchical assemblies have been found to be effective in producing photocurrent when they are anchored onto the electrode of a photoelectrochemical cell.[20] Herein we employed the I_3^-/I^- redox couple to regenerate the sensitizer. Photocurrent measurements were performed in a standard three-compartment cell as the working electrode along with a Pt wire gauze counterelectrode and a saturated calomel reference electrode (SCE). Figure 6A shows the photocurrent response of OTE/SnO_2/(H-H_2P-COO-TiO_2Tube+C_{60})$_n$ under illumination of white light. The photocurrent response was prompt, steady, and reproducible during repeated on/off cycles of visible-light illumination (more than five times). A photocurrent density (I_{sc}) of 1.4 mA cm^{-2} was reproducibly obtained during these measurements. Blank experiments conducted with OTE/SnO_2 (i.e., by excluding composite clusters (porphyrin-modified TiO_2+C_{60})$_n$) produced no detectable photocurrent under similar experimental conditions. These experiments confirmed the role of (porphyrin-modified TiO_2+C_{60})$_n$ assemblies in harvesting light energy and generating photocurrent during the operation of a photoelectrochemical cell. The I–V characteristics for one such assembly, H-H_2P bound to TiO_2 nanotubes and nanoparticles, are presented in Figure 6B to compare the I_{sc} values of three types of H-H_2P-COO-TiO_2-modified films. The photocurrent increased as the applied potential was scanned towards more-positive potentials. Increased charge separation and the facile transport of charge carriers under positive bias are responsible for enhanced photocurrent generation. At potentials greater than +0.4 V vs. SCE, direct electrochemical oxidation of iodide interfered with the photocurrent measurement. The observed current was a maximum when the applied anodic bias facilitated the charge separation and charge transport within the film. The H-H_2P–C_{60} assemblies bound to nanotubes exhibited superior performance in delivering higher photocurrent.[30]

To examine further the detailed photoelectrochemical properties, we also measured the incident photon-to-photocurrent efficiency (IPCE). The IPCE values were calculated by normalizing the photocurrent values for incident light energy and intensity with [Eq. (1)]:[22]

$$\text{IPCE}\ (\%) = 100 \times 1240 \times I_{sc}/(I_{inc} \times \lambda) \qquad (1)$$

where I_{sc} is the short-circuit photocurrent ($A\,cm^{-2}$), I_{inc} is the incident light intensity ($W\,cm^{-2}$), and λ is the wavelength (nm). Figure 7A and B show the IPCE spectra for H-H_2P and Ar-H_2P moieties anchored to TiO_2 nanoparticles or nanotubes. The IPCE response was rather broad with maximum performance in the 400–500-nm regions and overall response stretching up to 700 nm. The CT absorption between porphyrins and fullerenes mainly contributed to the photocurrent generation response (see above). The difference between the IPCE and absorption spectra in the long-wavelength region may have resulted from the scattering effect. The supramolecular assemblies anchored to the TiO_2 nanotubes produced a significantly higher IPCE than those with

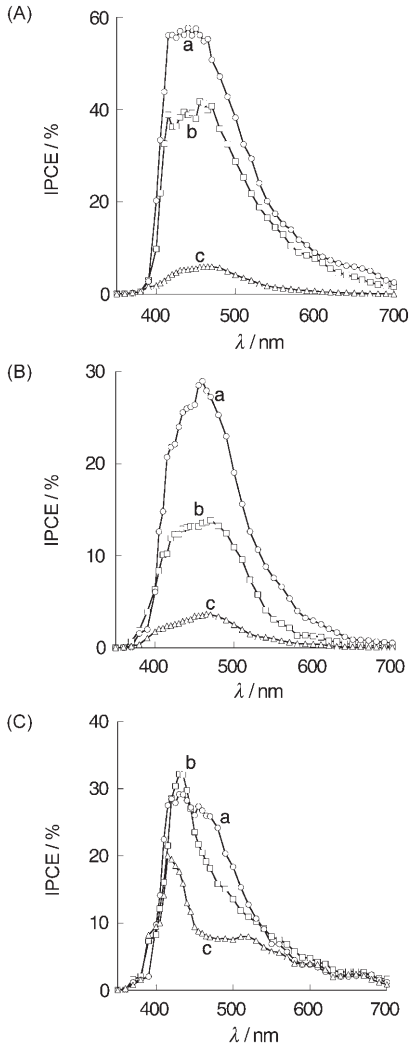

Figure 7. (A) Photocurrent action spectra of a) OTE/SnO_2/(H-H_2P-COO-TiO_2Tube + $C_{60})_n$, b) OTE/SnO_2/(H-H_2P-COO-TiO_2Pa + $C_{60})_n$, and c) OTE/SnO_2/(H-H_2P-COO-TiO_2Pa)$_n$ at an applied bias potential of 0.2 V vs. SCE. (B) Photocurrent action spectra of a) OTE/SnO_2/(Ar-H_2P-COO-TiO_2Tube + $C_{60})_n$, b) OTE/SnO_2/(Ar-H_2P-COO-TiO_2Pa + $C_{60})_n$, and c) OTE/SnO_2/(Ar-H_2P-COO-TiO_2Pa + $C_{60})_n$ at an applied bias potential of 0.2 V vs. SCE. (C) Photocurrent action spectra of a) OTE/SnO_2/(H_2P-4COO-TiO_2Tube + $C_{60})_n$, b) OTE/SnO_2/(H_2P-4COO-TiO_2Pa + $C_{60})_n$, and c) OTE/SnO_2/(H_2P-4COO-TiO_2Pa)$_n$ at an applied bias potential of 0.2 V vs. SCE. [H_2P] = 0.025 mM, [C_{60}] = 0.13 mM.

TiO_2 nanoparticles. The H-H_2P–C_{60} assemblies anchored to the TiO_2 nanotubes exhibited a maximum efficiency of about 60%. The Ar-H_2P–C_{60} assemblies showed a similar trend but with relatively low IPCE.

The interaction of C_{60} with the porphyrin moieties to form supramolecular assemblies for photoinduced charge separation is an important factor in attaining higher IPCEs in addition to the resulting hole and electron transport in the thin film. The insertion of C_{60} between two porphyrin rings of the porphyrin assembly on the TiO_2 surface becomes less favorable when *meso* positions are fully substituted in the Ar-H_2P-COO-TiO_2Tube system. The results described herein illustrate the importance of a favorable geometry obtained with H-H_2P and C_{60} assemblies. This argument is further supported by the fact that the IPCE values become significantly lower if we exclude C_{60} (Figure 7A and B, spectrum c). Furthermore, comparison of the IPCE values in the presence and absence of TiO_2 shows that the molecular organizations between donor and acceptor moieties with TiO_2 semiconductor nanomaterials are efficient for light-energy conversion (see Supporting Information S1).

The multipoint anchoring possibility of the tetracarboxylic acid substituted porphyrin (H_2P-4COOH) provides a large target on the TiO_2 surface and renders a planar geometry for the porphyrin moiety.[31] Complexation of H_2P-4COOH with C_{60} and its hierarchical organization on the electrode surface resulted in a configuration that is more different than that obtained with a single carboxylic acid linker because of multipoint anchors to the TiO_2 surface. Interestingly, the IPCE spectra of the H_2P-4COOH systems obtained for nanoparticles and nanotubes (Figure 7C) show comparable behavior with maximum IPCE of around 30%. In the planar geometry, the porphyrin molecules are closer to the TiO_2 surface, and the difference in the support structure has little effect on the maximum IPCE. The maximum photoresponse around 440 nm is broader for the tubes than the particles, which suggests stronger CT interactions on the tubular TiO_2 surface. The higher IPCE of the porphyrin-modified TiO_2 films (i.e., in the absence of C_{60}) suggests that deactivation by the charge-injection process is quite effective when the porphyrin moieties lie parallel to the TiO_2 surface, and the CT interaction in the excited porphyrin and C_{60} may be a contributing factor in the overall decrease in IPCE.

Mechanism of Photocurrent Generation

Characterization of the charge-injection events from the excited state of porphyrin into the TiO_2 nanoparticles have been presented in earlier studies.[6–10] The photocurrent arising from different derivatives of porphyrins in mesoporous TiO_2 films show sufficiently high IPCE values. Because of the random orientation of the sensitizer molecules on the particulate surface, it is difficult to assess the importance of geometrical orientation on the TiO_2 surface. By making use of the single and multi carboxylic acid functionality of porphyrins, we systematically assembled the supramolecular assemblies of TiO_2–porphyrin–C_{60} first and then deposited

them onto the electrodes (Figure 5). The planar and perpendicular orientations of porphyrins on the TiO_2 surface facilitate two different configurations for achieving supramolecular assemblies.

The IPCE values for different supramolecular organizations (Figure 7) show the importance of the orientation of assemblies of TiO_2–porphyrin–C_{60} on the electrode surface. An added feature in the present system is the introduction of C_{60} to complex with porphyrins to aid in the organization of molecules as supramolecular assemblies. Furthermore, C_{60} is capable of playing the role of an electron relay and facilitating charge transport across the film.[32] In all three examples presented in Figure 7, we observed a significantly higher IPCE when C_{60} is present along with porphyrin. The possibility exists for porphyrin to undergo CT interaction with C_{60} and generate the $C_{60}^{\bullet-}$ ion. If this is a dominant process, it is necessary for $C_{60}^{\bullet-}$ to transfer electrons to TiO_2 to generate the photocurrent in a photogalvanic mode.[23,33] However, the conduction band of TiO_2 is about 0.5 V versus a normal hydrogen electrode (NHE), which is more negative than the reduction potential of the $C_{60}/C_{60}^{\bullet-}$ couple ($\approx$0.2 V vs. NHE); this electron-transfer process is thus energetically unfavorable. Earlier studies[23,32] carried out with C_{60}-modified SnO_2 and TiO_2 electrodes have established that $C_{60}^{\bullet-}$ can transfer electrons only to SnO_2 and not to TiO_2 (Figure 8). The fact that we were able to see significant

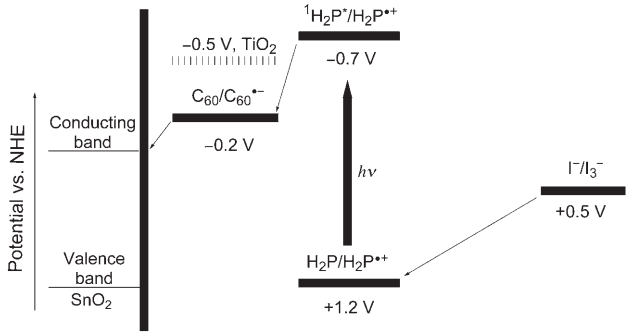

Figure 8. Mechanism of photocurrent generation in the TiO_2–porphyrin–C_{60} assembly system.

IPCE values with porphyrin–C_{60}-modified TiO_2 films (Figure 7) shows that interaction between excited porphyrin and TiO_2 plays a dominant role in photocurrent generation.

As established earlier,[10] the primary event following the excitation of porphyrin is the injection of electrons directly into the TiO_2 nanotubes or nanoparticles, which are then transported to the electrode surface to generate the photocurrent. In the absence of C_{60}, one would expect the regeneration of the sensitizer to occur by charge transfer from the I^- species present in the electrolyte. However, in the presence of C_{60} and iodide ions, $C_{60}^{\bullet-}$ can quickly accumulate in the film and mediate the regeneration process.[34]

As shown earlier,[23,32] when C_{60} is excited with red-wavelength photons, it undergoes electron transfer with I^- to produce $C_{60}^{\bullet-}$. The $C_{60}/C_{60}^{\bullet-}$ couple plays the role of an electron shuttle and facilitates quick regeneration of the sensitizer. The higher IPCE values observed with the inclusion of C_{60} supports its beneficial role in attaining favorable supramolecular assemblies on the electrode surface.

Power-Conversion Efficiency of OTE/SnO_2/(H-H_2P-COO-TiO_2Tube + C_{60})$_n$ Electrode

We also determined the power-conversion efficiency (η) of the photoelectrochemical cell by varying the load resistance (Figure 9). A drop in the photovoltage and an increase in

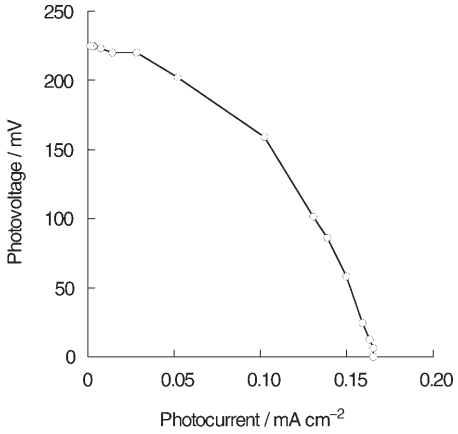

Figure 9. Power characteristics of OTE/SnO_2/(H-H_2P-COO-TiO_2Tube + C_{60})$_n$ ([H_2P] = 0.025 mM, [C_{60}] = 0.13 mM) under white-light illumination ($\lambda > 400$ nm); electrolyte: 0.5 M NaI and 0.01 M I_2 in acetonitrile; input power: 3.4 mW cm^{-2}.

the photocurrent were observed with a decrease in the load resistance. Power-conversion efficiency (η) is calculated by [Eq. (2)]:[22]

$$\eta = \mathrm{FF} \times I_{sc} \times V_{oc}/W_{in} \quad (2)$$

where the fill factor (FF) is defined as $\mathrm{FF} = (IV)_{max}/I_{sc}V_{oc}$, V_{oc} is the open circuit photovoltage, and W_{in} is the input power.

The OTE/SnO_2/(H-H_2P-COO-TiO_2Tube + C_{60})$_n$ system has a much larger FF of 0.44, a V_{oc} value of 230 mV, and an I_{sc} value of 0.16 mA cm^{-2}, and an overall η of 0.51% at a W_{in} value of 3.4 mW cm^{-2}. Furthermore, the η value of organized OTE/SnO_2/(H-H_2P-COO-TiO_2Tube + C_{60})$_n$ with TiO_2 nanoparticles is more than 10 times larger than that of a nonorganized composite cluster system of porphyrin and fullerene without TiO_2 nanoparticles, which was reported previously ($\approx$0.03%).[22]

Conclusions

We have constructed shape- and functionality-controlled photochemical solar cells by using hierarchical organization of porphyrin derivatives–C_{60} assemblies. By employing TiO_2 nanotubes and nanoparticles, we succeeded in varying the

three-dimensional organization of the supramolecular assemblies. The drastic differences in the efficiency of light-energy conversion demonstrate the importance of the geometrical orientation of the porphyrins with respect to the TiO_2 surface and the resulting supramolecular organization of the porphyrin and C_{60} moieties. The maximum IPCE of 60% obtained with TiO_2 nanotubes is indicative of the fact that nanotubes are better suited for anchoring porphyrin moieties and promoting electron transport within the mesoscopic semiconductor film.

Experimental Section

General

Chemicals used in this study were of the best grade available, supplied by Tokyo Chemical Industries, Wako Pure Chemical, or Sigma Aldrich Co. ^{1}H NMR spectra were recorded on a JNM-AL300 (JEOL) instrument at 300 MHz. Matrix-assisted laser desorption/ionization (MALDI) time-of-flight (TOF) mass spectra were recorded on a Kratos Compact MALDI I (Shimadzu) spectrometer. TiO_2 nanoparticles (P25, $d = 21$ nm) were purchased from Nippon Aerogel Co.

Preparation of Porphyrin-Modified TiO_2 Nanomaterials

The TiO_2 nanoparticles and nanotubes prepared by literature methods[35,36] were functionalized with three different carboxylic acid derivatives of porphyrins as illustrated in Figure 5. The preparation of Ar-H_2P-COOH and H-H_2P-COOH have been described elsewhere.[37,38] H_2P-4COOH was purchased from Sigma Aldrich Co. TiO_2 nanotubes and nanoparticles modified with porphyrin moieties (Ar-H_2P-COO-TiO_2Tube, H-H_2P-COO-TiO_2Tube, H_2P-4COO-TiO_2Tube, Ar-H_2P-COO-TiO_2Pa, H-H_2P-COO-TiO_2Pa, and H_2P-4COO-TiO_2Pa) were prepared by immersing warmed TiO_2 nanotubes or nanoparticles (80–100 °C) in acetonitrile (10 mL) containing 3.0×10^{-4} M of Ar-H_2P-COOH, H-H_2P-COOH, or H_2P-4COOH, respectively, for 12 h. After adsorbing Ar-H_2P-COOH, H-H_2P-COOH, or H_2P-4COOH, the TiO_2 nanotubes or nanoparticles were filtered, and subsequent washing with acetonitrile and drying afforded Ar-H_2P-COO-TiO_2Tube or Ar-H_2P-COO-TiO_2Pa, H-H_2P-COO-TiO_2Tube or H_2P-COO-TiO_2Pa, and H_2P-4COO-TiO_2Tube or H_2P-4COO-TiO_2Pa, respectively. The dye molecules were completely desorbed from the TiO_2 nanotubes or nanoparticles into solution by immersing the dye-modified TiO_2 nanotubes or nanoparticles in methanol overnight. The amounts of Ar-H_2P-COOH, H-H_2P-COOH, and H_2P-4COOH adsorbed onto the TiO_2 nanotubes or nanoparticles relative to the total weight were determined as 3.00×10^{-5} or 2.98×10^{-5}, 3.00×10^{-5} or 2.98×10^{-5}, and 3.00×10^{-5} or 2.97×10^{-5} mol g^{-1}, respectively. As the average surface areas of the TiO_2 nanoparticles and nanotubes were approximately the same as those reported in a previous study,[36] we considered the distance between two porphyrins to be the same in both cases (≈17.5 Å). This value is quite suitable for the accommodation of C_{60} between two porphyrins according to our previous result.[20]

Fabrication of Composite Films

C_{60} is soluble in nonpolar solvents such as toluene. In mixed solvents (acetonitrile/toluene), however, they aggregate to form large clusters with diameters of around 100 nm.[22] The C_{60} clusters and TiO_2 nanotubes and nanoparticles were electrophoretically deposited onto SnO_2 films under an applied potential as reported previously.[22] Nanostructured SnO_2 films were cast on an OTE by using a dilute (1–2%) colloidal solution (Alfa Chemicals). The dried film was then annealed at 673 K. Details of the preparation of the electrode and its properties have been described elsewhere.[39] These films are highly porous and electrochemically active; charges can be conducted across the films. The SnO_2 film electrode (OTE/SnO_2) and an OTE plate were introduced in a cuvette of 1-cm path length and were connected to the positive and negative terminals of the power supply, respectively. A known amount (≈2 mL) of C_{60}, porphyrin-modified TiO_2 nanoparticles (Ar-H_2P-COO-TiO_2, H-H_2P-COO-TiO_2, and H_2P-4COO-TiO_2), or the mixed cluster suspension in acetonitrile/toluene (3:1 *v/v*) was transferred immediately after ultrasonication to a 1-cm cuvette in which the two electrodes (OTE/SnO_2 and OTE) were kept at a distance of about 6 mm by using a teflon spacer. A dc electric field (≈500 V cm^{-1}) was applied between the two electrodes for 2 min with a Fluke 415 power supply. The deposition of the film was visibe as the solution became colorless with simultaneous brown coloration of the SnO_2/OTE electrode. Within 2–3 min, the organized supramolecular assemblies of (porphyrin-modified $TiO_2+C_{60})_n$ were driven to the OTE surface to form a dark film.

Measurement of Photoelectrochemical Properties

Photoelectrochemical measurements were performed by using a standard three-compartment cell consisting of a working electrode, a Pt wire gauze counterelectrode, and an SCE. All photoelectrochemical measurements were carried out in acetonitrile containing NaI (0.5 mol dm^{-3}) and I_2 (0.01 mol dm^{-3}) with a Keithley Model 617 programmable electrometer. A collimated light beam from a 150-W xenon lamp with a 400-nm cut-off filter was used for excitation of the composite cluster films cast on the SnO_2 electrodes. A Bausch and Lomb high-intensity grating monochromator was introduced into the path of the excitation beam for wavelength selection. A Princeton Applied Research (PAR) Model 173 potentiostat and Model 175 universal programmer were used for recording *I–V* characteristics.

Acknowledgements

This work was partially supported by a Grant-in-Aid from the Ministry of Education, Culture, Sports, Science, and Technology, Japan. We thank Mr. Yoshinori Ohsaki (Osaka University) and Prof. Yuji Wada (Okayama University) for providing us with TiO_2 nanotubes. P.V.K. acknowledges support from the Office of Basic Energy Science, U.S. Department of Energy. This is contribution No. NDRL 4667 from the Notre Dame Radiation Laboratory.

[1] M. Grätzel, *Inorg. Chem.* **2005**, *44*, 6841.
[2] K. Hara, T. Horiguchi, T. Kinoshita, K. Sayama, H. Sugihara, H. Arakawa, *Sol. Energy Mater. Sol. Cells* **2000**, *64*, 115.
[3] A. Hagfeldt, M. Grätzel, *Chem. Rev.* **1995**, *95*, 49.
[4] M. Adachi, Y. Murata, I. Okada, S. Yoshikawa, *J. Electrochem. Soc.* **2003**, *150*, G488.
[5] K. Tennakone, G. K. R. Senadeera, D. B. R. A. De Silva, I. R. M. Kottegoda, *Appl. Phys. Lett.* **2000**, *77*, 2367.
[6] G. K. Boschloo, A. Goossens, *J. Phys. Chem.* **1996**, *100*, 19489.
[7] A. Brune, G. Jeong, P. A. Liddell, T. Sotomura, T. A. Moore, A. L. Moore, D. Gust, *Langmuir* **2004**, *20*, 8366.
[8] S. Cherian, C. C. Wamser, *J. Phys. Chem. B* **1999**, *104*, 3624.
[9] T. J. Savenije, E. Moons, G. K. Boschloo, A. Goossens, T. J. Schaafsma, *Phys. Rev. B* **1997**, *55*, 9685.
[10] Y. Tachibana, S. A. Haque, I. P. Mercer, J. R. Durrant, D. R. Klug, *J. Phys. Chem. B* **2000**, *104*, 1198.
[11] Q. Wang, W. M. Campbell, E. E. Bonfantani, K. W. Jolley, D. L. Officer, P. J. Walsh, K. Gordon, R. Humphry-Baker, M. K. Nazeeruddin, M. Grätzel, *J. Phys. Chem. B* **2005**, *109*, 15397.
[12] A. Kay, M. Grätzel, *J. Phys. Chem.* **1993**, *97*, 6272.
[13] P. G. Hoertz, R. A. Carlisle, G. J. Meyer, D. Wang, P. Piotrowiak, E. Galoppini, *Nano Lett.* **2003**, *3*, 325.
[14] D. Wang, R. Mendelsohn, E. Galoppini, P. G. Hoertz, R. A. Carlisle, G. J. Meyer, *J. Phys. Chem. B* **2004**, *108*, 16642.
[15] P. D. W. Boyd, M. C. Hodgson, C. E. F. Rickard, A. G. Oliver, L. Chaker, P. J. Brothers, R. D. Bolskar, F. S. Tham, C. A. Reed, *J. Am. Chem. Soc.* **1999**, *121*, 10487.
[16] H. Imahori, K. Yamada, M. Hasegawa, S. Taniguchi, T. Okada, Y. Sakata, *Angew. Chem.* **1997**, *109*, 2740; *Angew. Chem. Int. Ed. Engl.* **1997**, *36*, 2626.

[17] P. A. Liddell, J. P. Sumida, A. N. MacPherson, L. Noss, G. R. Seely, K. N. Clark, A. L. Moore, T. A. Moore, D. Gust, *Photochem. Photobiol.* **1994**, *60*, 537.
[18] T. Hasobe, S. Hattori, H. Kotani, K. Ohkubo, K. Hosomizu, H. Imahori, P. V. Kamat, S. Fukuzumi, *Org. Lett.* **2004**, *6*, 3103.
[19] T. Hasobe, H. Imahori, S. Fukuzumi, P. V. Kamat, *J. Am. Chem. Soc.* **2003**, *125*, 14962.
[20] T. Hasobe, H. Imahori, P. V. Kamat, S. Fukuzumi, *J. Am. Chem. Soc.* **2005**, *127*, 1216.
[21] T. Hasobe, P. V. Kamat, M. A. Absalom, Y. Kashiwagi, J. Sly, M. J. Crossley, K. Hosomizu, H. Imahori, S. Fukuzumi, *J. Phys. Chem. B* **2004**, *108*, 12865.
[22] T. Hasobe, H. Imahori, S. Fukuzumi, P. V. Kamat, *J. Phys. Chem. B* **2003**, *107*, 12105.
[23] P. V. Kamat, S. Barazzouk, K. George Thomas, S. Hotchandani, *J. Phys. Chem. B* **2000**, *104*, 4014.
[24] T. Miyasaka, Y. Kijitori, T. N. Murakami, M. Kimura, S. Uegusa, *Chem. Lett.* **2002**, *31*, 1250.
[25] D. Zhang, T. Yoshida, H. Minoura, *Adv. Mater.* **2003**, *15*, 814.
[26] D. Zhang, T. Yoshida, H. Minoura, *Chem. Lett.* **2002**, *31*, 874.
[27] H. Imahori, N. V. Tkachenko, V. Vehmanen, K. Tamaki, H. Lemmetyinen, Y. Sakata, S. Fukuzumi, *J. Phys. Chem. A* **2001**, *105*, 1750.
[28] N. V. Tkachenko, C. Guenther, H. Imahori, K. Tamaki, Y. Sakata, S. Fukuzumi, H. Lemmetyinen, *Chem. Phys. Lett.* **2000**, *326*, 344.
[29] N. V. Tkachenko, H. Lemmetyinen, J. Sonoda, K. Ohkubo, T. Sato, H. Imahori, S. Fukuzumi, *J. Phys. Chem. A* **2003**, *107*, 8834.
[30] IPCE values of OTE/SnO_2/(H-H_2P-COO-TiO_2Tube+C_{60})$_n$, OTE/SnO_2/(H-H_2P-COO-TiO_2Pa+C_{60})$_n$, and OTE/SnO_2/(H-H_2P-COOMe+C_{60})$_n$ with no applied potential were also observed. The IPCE values of OTE/SnO_2/(H-H_2P-COO-TiO_2Tube+C_{60})$_n$ and OTE/SnO_2/(H-H_2P-COO-TiO_2Pa+C_{60})$_n$ were much higher than that of the nonorganized assembly system of OTE/SnO_2/(H-H_2P-COOMe+C_{60})$_n$; see Supporting Information, Figure S1.
[31] In the multipoint anchor system, two-point or four-point connections may take place on the TiO_2 surface. More-complicated structures are also possible because of the strong aggregation of the molecular assemblies in mixed solvents.
[32] P. V. Kamat, M. Haria, S. Hotchandani, *J. Phys. Chem. B* **2004**, *108*, 5166.
[33] D. W. Thompson, C. A. Kelly, F. Farzad, G. J. Meyer, *Langmuir* **1999**, *15*, 650.
[34] The maximum IPCE value (≈20%) was obtained for OTE/SnO_2/(H_2P-4COO-TiO_2Pa)$_n$, which is much larger than those of OTE/SnO_2/(Ar-H_2P-COO-TiO_2)$_n$ (≈3.5%) and OTE/SnO_2/(H-H_2P-COO-TiO_2Pa)$_n$ (≈6%). From the structural point of view between porphyrin moieties and TiO_2 nanoparticles, the porphyrin moieties definitely lie on the TiO_2 surface because of multipoint connections in the case of OTE/SnO_2/(H_2P-4COO-TiO_2Pa)$_n$, whereas these moieties may stand on the TiO_2 surface in the cases of OTE/SnO_2/(Ar-H_2P-COO-TiO_2)$_n$ and OTE/SnO_2/(H-H_2P-COO-TiO_2)$_n$ as shown in Figure 5.
[35] T. Kasuga, M. Hiramatsu, A. Hoson, T. Sekino, K. Niihara, *Adv. Mater.* **1999**, *11*, 1307.
[36] Y. Ohsaki, N. Masaki, T. Kitamura, Y. Wada, T. Okamoto, T. Sekino, K. Niihara, S. Yanagida, *Phys. Chem. Chem. Phys.* **2005**, *7*, 4157.
[37] H. Yamada, H. Imahori, Y. Nishimura, I. Yamazaki, T. K. Ahn, S. K. Kim, D. Kim, S. Fukuzumi, *J. Am. Chem. Soc.* **2003**, *125*, 9129.
[38] T. Hasobe, H. Imahori, H. Yamada, T. Sato, K. Ohkubo, S. Fukuzumi, *Nano Lett.* **2003**, *3*, 409.
[39] I. Bedja, S. Hotchandani, P. V. Kamat, *J. Phys. Chem.* **1994**, *98*, 4133.

Received: October 23, 2006
Published online: January 9, 2007

